A Cobalt(III) Chiroporphyrin and Its Amine Adducts. A Potential Chiral NMR Shift Reagent for Amines

Dawn Toronto,[†] Françoise Sarrazin,[†] Jacques Pécaut,[†] Jean-Claude Marchon,*[,†] Maoyu Shang,[‡] and W. Robert Scheidt*[,‡]

Département de Recherche Fondamentale sur la Matière Condensée/SCIB, Laboratoire de Chimie de Coordination (URA CNRS 1194), CEA-Grenoble, 38054 Grenoble, France, and Department of Chemistry and Biochemistry, University of Notre Dame, Notre Dame, Indiana 46556

Received August 7, 1997

The chlorocobalt(III) complex of $\alpha\beta\alpha\beta$-tetramethylchiroporphyrin, CoCl(TMCP), has been prepared as a potential enantioselective host or chiral NMR shift reagent for optically active amines. The X-ray structure of CoCl-($OHCH_2CH_3$)(TMCP) shows the six-coordinate cobalt(III) ion at the center of a strongly ruffled porphyrin. The 2-fold-disordered ethanol ligand interacts with the chiroporphyrin host by two C−H···O hydrogen bonds to the carbonyl groups of two ester substituents. Primary amines bind to this diamagnetic cobalt(III) center to form cationic 2:1 complexes in which the ^{1}H NMR resonances of the axial ligands are shifted upfield of tetramethylsilane by the porphyrin ring current. Coordinated enantiopure 2-alkylamines exhibit NMR signals for the protons of the amine group which are characteristic of their (*R* or *S*) absolute configuration. The bis-complexes of the same amines in racemic form exist as three different species, (*R*,*R*), (*S*,*S*), and (*R*,*S*), in 1:1:2 relative ratios. Negligible enantioselection by the chiral host suggests kinetic control of bis(amine) complex formation on cobalt(III). The X-ray structure of the bis((*S*)-2-butylamine) complex $[Co((S)\text{-}NH_2CH(CH_3)CH_2CH_3)_2(TMCP)][CoCl_4]_{0.5}$ shows a 2-fold-disordered amine on one face of the porphyrin only. The unique amine on the other face is held within the porphyrin groove by a network of weak interactions including N−H···O and C−H···O hydrogen bonds. With its ability to induce good resolution of axial ligand ^{1}H NMR resonances and slow dissociation kinetics of its bis-adducts, CoCl(TMCP) may be useful as a chiral NMR shift reagent for conformational studies of chiral amines and as an analytical reagent for the determination of their enantiomer composition.

Introduction

Chiral metalloporphyrins are believed to have a considerable potential as asymmetric catalysts[1] and enantioselective receptors of optically active ligands,[2] and their design is the focus of active current interest in the context of enantioselective synthesis and of molecular and chiral recognition research.[3] Our approach to C_2-symmetric metalloporphyrins is to attach bulky substituents on chiral centers near the plane of the tetrapyrrolic ring, as close as possible to the metal atom to maximize steric interaction with incoming substrate.[4] We have shown that a chiroporphyrin catalyst possessing these topological features can be easily constructed from a chiral cyclopropanecarbaldehyde derivative.[5] The prototypic tetramethylchiroporphyrin, TMCPH$_2$, can be obtained from (1*R*)-*cis*-caronaldehydic acid methyl ester and pyrrole as the desired D_2-symmetric $\alpha\beta\alpha\beta$ atropisomer, **1**, which exhibits a groove along a *meso* diagonal on each face of the macrocycle. This chiroporphyrin unit also exhibits multipoint binding properties with potentially important applications in chiral recognition of alcohols. Thus, recent studies in these laboratories have shown that the carbonylruthenium(II) tetramethylchiroporphyrin complex discriminates enantiomers of chiral aliphatic alcohols in solution at −70 °C. The upfield-shifted ^{1}H NMR resonances of the bound alcohol enantiomers are resolved at 400 MHz, and they reflect substantial enantioselection by the chiral host (*R*:*S* = *ca.* 2.2 for 2-octanol).[6] However, the practical utility of this ruthenium-based receptor in alcohol enantioselection appears to be restricted to low temperatures by weak axial ligand binding and high kinetic lability at room temperature. In order to design a room-temperature NMR chiral shift reagent or enantioselective

[†] CEA-Grenoble.
[‡] University of Notre Dame.

(1) For recent reviews, see: (a) Collman, J. P.; Zhang, X.; Lee, V. J.; Uffelman, E. S.; Brauman, J. I. *Science* **1993**, *261*, 1404. (b) Naruta, Y. In *Metalloporphyrins in Catalytic Oxidations*; Sheldon, R. A., Ed.; Marcel Dekker: New York, 1994; p 241. (c) Campbell, L. A.; Kodadek, T. *J. Mol. Catal. A* **1996**, *113*, 293. (d) Suslick, K. S.; Van Deusen-Jeffries, S. In *Comprehensive Supramolecular Chemistry*; Atwood, J. L., Davies, J. E. D., MacNicol, D. D., Vögtle, F., Lehn, J. M., Eds.; Elsevier: Oxford, U.K., 1996; Vol. 5, p 337.

(2) For recent reviews, see: (a) Rebek, J. *Angew. Chem., Int. Ed. Engl.* **1990**, *29*, 245. (b) Izatt, R. M.; Bradshaw, J. S.; Pawlak, K.; Bruening, R. L.; Tarbet, B. J *Chem. Rev.* **1992**, *92*, 1261. (c) Ogoshi, H.; Mizutani, T. In *Comprehensive Supramolecular Chemistry*; Atwood, J. L., Davies, J. E. D., MacNicol, D. D., Vögtle, F., Lehn, J. M., Eds.; Elsevier: Oxford, U.K., 1996; Vol. 4, p 141. (d) Canary, J. W.; Gibb, B. C. *Prog. Inorg. Chem.* **1997**, *45*, 1.

(3) For recent reviews, see: (a) Lehn, J. M. *Angew. Chem., Int. Ed. Engl.* **1988**, *27*, 89. (b) Cram, D. J. *Angew. Chem., Int. Ed. Engl.* **1988**, *27*, 1009. (c) *Frontiers in Supramolecular Organic Chemistry and Photochemistry*; Schneider, H. J., Dürr, H., Eds.; VCH: Weinheim, Germany, 1990. (d) Vögtle, F. *Supramolecular Chemistry, an Introduction*; John Wiley & Sons: New York, 1991. (e) *Molecular Recognition* (Tetrahedron Symposia No. 56); Hamilton, A. D., Ed.; *Tetrahedron* **1995**, 51. (f) Webb, T. H.; Wilcox, C. S. *Chem. Soc. Rev.* **1993**, 383.

(4) Pfaltz, A. *Acc. Chem. Res.* **1993**, *26*, 339.

(5) Veyrat, M.; Maury, O.; Faverjon, F.; Over, D. E.; Ramasseul, R.; Marchon, J. C.; Turowska-Tyrk, I.; Scheidt, W. R. *Angew. Chem., Int. Ed. Engl.* **1994**, *33*, 220.

(6) Mazzanti, M.; Veyrat, M.; Ramasseul, R.; Marchon, J. C.; Turowska-Tyrk, I.; Shang, M.; Scheidt, W. R. *Inorg. Chem.* **1996**, *35*, 3733.

S0020-1669(97)00995-6 CCC: $15.00
Published on Web 01/22/1998

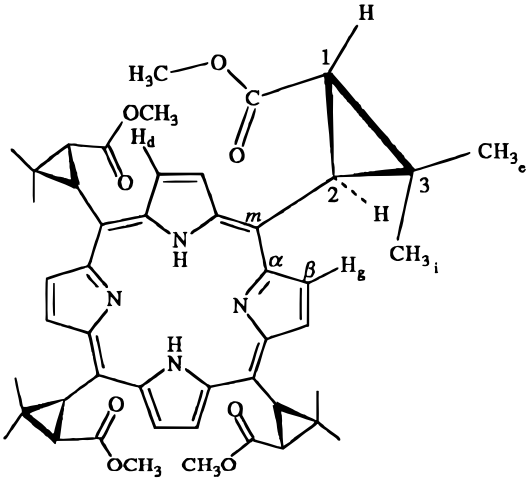

1

metalloreceptor, it appeared desirable to include in the tetramethylchiroporphyrin unit an inert, diamagnetic metal center, such as cobalt(III), which would exhibit slower axial ligand exchange kinetics. We were encouraged in this approach by Gaudemer's and Abraham's studies on cobalt(III) tetraphenylporphyrin and cobalt(III) octaethylporphyrin, which demonstrated that these complexes are useful NMR shift reagents for amines at room temperature.[7] In this paper, we report the synthesis and structural characterization of the diamagnetic chlorocobalt(III) tetramethylchiroporphyrin, CoCl(TMCP) (**2**). We show that chiral aliphatic amines bind to this cobalt center to form bis(amine) cationic complexes which are kinetically inert on the NMR time scale at room temperature. A plausible conformation for the coordinated amines in solution is proposed on the basis of their upfield-shifted ^{1}H NMR resonances and of the crystal structure of the bis(*(S)*-2-butylamine) complex. Finally, the potential of these chiral porphyrin shift reagents in the analysis of mixtures of amine enantiomers is discussed.

Experimental Section

Materials. Tetramethylchiroporphyrin was prepared according to a procedure worked out earlier in our laboratories.[8] The chiral amines 2-butylamine (*(R), (S),* and *(R,S)*), *(R,S)*-2-pentylamine, and *(R,S)*-2-heptylamine were purchased from Fluka and used without further purification.

Synthesis of CoCl(TMCP). To 75 mg (0.092 mmol) of tetramethylchiroporphyrin dissolved in 15 mL of chloroform was added 119 mg (0.920 mmol) of $CoCl_2$ dissolved in 7 mL of ethanol. Within a period of 30 min the purple solution turns red/green. The metal insertion was checked by monitoring the visible spectrum of an aliquot of the chloroform/ethanol solution. After the solution was stirred for 12 h the volume was reduced to dryness, the residue taken up in dichloromethane, and the solution filtered over a thin bed of Celite. Addition of hexanes precipitated a red/green powder containing the Co(III) complex and unreacted $CoCl_2$. The crude product was dissolved in 7 mL of dichloromethane and passed through a second short bed of Celite after which crystallization by addition of hexanes afforded red/green crystals of CoCl(TMCP), **2**, in 87% yield: ^{1}H NMR (CD_2Cl_2, 200 MHz) δ = 9.34 (m, J = 5 Hz, 4 H; pyrrole H), 9.22 (m, J = 5 Hz, 4 H; pyrrole H), 4.73 (d, J = 10 Hz, 2H; H_2), 4.66 (d, J = 10 Hz, 2H; H_2), 3.19 (s, 6H; OCH_3), 2.97 (s, 6H; OCH_3), 2.72 (d, J = 10 Hz, 2H; H_1) 2.59 (d, J = 10 Hz, 2H; H_1), 1.9 (s, 6H; CH_3), 1.86 (s, 6H; CH_3), 0.51 (s, 6H; CH_3), 0.41 (s, 6H; CH_3); UV/vis (CH_2Cl_2) λ_{max} 449, 570, 612 nm; FAB-MS (3-nitrobenzyl alcohol) m/z 871 ($M^+ - Cl$).

General Spectroscopic Information. UV/vis spectra were recorded on a Perkin-Elmer Lambda 9. ^{1}H NMR spectra were recorded on either a Varian 400 or a Bruker 200 MHz NMR spectrometer. Parameters for acquiring proton spectra were the following: Bruker 200 MHz NMR, 15 accumulations, spectral window 6000 Hz, 16K data points, 90° pulse to give a digital resolution of 0.37 Hz per point; Varian 400 MHz NMR, 8 accumulations, spectral window 8785 Hz, 17.6 K data points, 90° pulse to give a digital resolution of 0.49 Hz per point. ^{1}H−^{1}H double-quantum-filtered COSY spectra (4032 points in time domain) were recorded with 32 scans and 256 t_1 increments using the pulse sequence (D_1, $\pi/2$, $\pi/2$, $\pi/2$, Acq), with a relaxation delay D_1 = 1 s, a 90° pulse of 12.2 μs, and an acquisition time of 0.3 s. Chemical shifts are reported to CD_2Cl_2.

^{1}H NMR Shift Studies of Amines. To a solution of 3.3 mg (0.003 mmol) of CoCl(TMCP) in CD_2Cl_2 (0.7 mL) was added 2 equiv (0.006 mmol) of the chiral amine 2-butylamine, 2-pentylamine, or 2-heptylamine (*(R), (S),* or *(R,S)*). The formation of the bis(amine) salt was immediate and was accompanied by a change in color from red to blue/green. ^{1}H NMR spectra were taken following the titration. These complexes were stable in solution, and no substantial change was observed in their ^{1}H NMR spectra after a period of several weeks. Single crystals of the [Co(*(S)*-2-butylamine)$_2$(TMCP)][$CoCl_4$]$_{0.5}$, **3**, complex were obtained by slow diffusion of *n*-hexane in 0.7 mL of a CD_2Cl_2 solution used for NMR studies.

X-ray Structure Determinations. CoCl(TMCP). A dark-green crystal of **2** (0.2 × 0.2 × 0.2 mm^3) was used for the structure determination. Data collection was carried out on a Siemens SMART diffractometer with a CCD detector at low temperature (173(2) K) with Mo radiation (λ = 0.710 73 Å). A first cell was obtained from 3 runs of 15 frames each; each frame corresponded to a 0.3° scan in 30 s. Intensities were then collected with 0.2° width frames exposed for 30 s. A total of 10 950 data were observed on 1120 frames. Cell parameters were refined on all data with the SAINT program.[9] Lorentz and polarization correction were made. Anisotropic absorption correction was necessary because of the 3-circle diffractometer geometry, and it was carried out with the SADABS program. The structure was solved with the direct methods program SHELXTL,[10] which revealed the porphyrin atoms. Difference Fourier synthesis led to the location of all the remaining non-hydrogen atoms. The structure refinement was performed on F^2. A disordered ethanol molecule was found on two symmetry-related axial sites with an occupancy of 0.5 for each location. The hydrogen atoms of the porphyrin ring were located and put on fixed positions. The ethanol hydrogen atoms could not be located, presumably because of the disorder of this ligand. Final atomic coordinates are listed in Table S2 (Supporting Information).

[Co(*(S)*-2-butylamine)$_2$(TMCP)][$CoCl_4$]$_{0.5}$. Single-crystal experiments for **3** were carried out on an Enraf-Nonius FAST area detector diffractometer at 130 K with our standard methods for small molecules.[11] A black crystal of [Co(*(S)*-$NH_2CH(CH_3)CH_2CH_3$)$_2$(TMCP)]-[$CoCl_4$]$_{0.5}$(H_2O)(C_6H_{14})$_{0.5}$(CH_2Cl_2)$_{0.27}$ with a refined effective mosaic spread of 0.518° was used for data collection. A brief summary of determined parameters is given in Table S1′. A total of 63 116

(7) (a) Gouedard, M.; Riche, C.; Gaudemer, A.; et al. *J Chem. Res. (S)* **1978**, *8*, 30, 32, 34, 36. (b) Gaudemer, A.; Gaudemer, F.; Merienne, C. *Org. Magn. Reson.* **1983**, *21*, 83. (c) Abraham, R. J.; Bedford, G. R.; Wright, B. *Org. Magn. Reson.* **1982**, *18*, 45. (d) Abraham, R. J.; Bedford, G. R.; Wright, B. *Org. Magn. Reson.* **1983**, *21*, 637. (e) Abraham, R. J.; Plant, J.; Bedford, G. R.; Wright, B. *Org. Magn. Reson.* **1984**, *22*, 57. (f) Abraham, R. J.; Medforth, C. J. *Magn. Res. Chem*. **1987**, *25*, 432. (g) Abraham, R. J.; Medforth, C. J. *J. Chem. Soc., Chem. Commun*. **1987**, 1637. (h) Abraham, R. J.; Medforth, C. J. *Magn. Res. Chem*. **1987**, *25*, 790. (i) Abraham, R. J.; Medforth, C. J. *Magn. Res. Chem*. **1988**, *26*, 334. (j) Abraham, R. J.; Medforth, C. J. *Magn. Res. Chem*. **1988**, *26*, 803. (k) Abraham, R. J.; Medforth, C. J. *Magn. Res. Chem*. **1990**, *28*, 343. (l) Abraham, R. J.; Marsden, I. *Tetrahedron* **1992**, *48*, 7489.

(8) Veyrat, M.; Fantin, L.; Desmoulins, S.; Petitjean, A.; Mazzanti, M.; Ramasseul, R.; Marchon, J. C.; Bau, R. *Bull. Soc. Chim. Fr*. **1997**, *134*, 703.

(9) *SMART and SAINT Area-Detector Control and Integration Software*; Siemens Analytical X-Ray Instruments Inc.: Madison, WI, 1995.

(10) Sheldrick, G. M. *SHELXTL-Plus, Version 5. Program for the Refinement of Crystal Structures*; University of Göttingen: Göttingen, Germany, 1994.

(11) Scheidt, W. R.; Turowska-Tyrk, I. *Inorg. Chem.* **1994**, *33*, 1314.

reflections were collected, of which 10 526 were unique and intensities of 5526 unique reflections were larger than $2\sigma(I)$. All reflections were reduced using Lorentz−polarization factors. No absorption correction was made except for averaging a large number of identical (collected at different azimuth angles) and equivalent reflections. The structure was solved by direct methods with the SHELXS-86 program.[12] The cobalt atom and most of the non-hydrogen atoms of the TMCP ligand were located on a sharpened *E*-map. Ensuing least-squares refinement and difference Fourier synthesis gradually revealed details of the remaining (disordered) structure. The butyl group of one amine ligand (C(61)−C(68)) was disordered on two locations with an occupancy ratio of *ca.* 2:1, and *ca.* $^1/_3$ of the β-carbon atom (C(63B)) of the primary position was further disordered. The packing inefficiency caused by this disorder was improved partially by filling the site with methylene dichloride at a location close to the secondary location of the disordered amine. Near the ordered amine (N(5)) site, a water molecule and a tetrachlorocobaltate counteranion were also found, the latter being disordered in a peculiar way. The cobalt atom was off a 2-fold axis by only 0.599(4) Å, so that the tetrachlorocobaltate was disordered around the 2-fold axis and each location has an occupancy of one-half. Further away from the 2-fold axis, a water molecule was assigned based on the electron density of the site. Away from the main part of the structure a few diffuse electron densities formed a chainlike region. Modeling these with several methylene chloride molecules with low occupancies gave an unusually wide range of thermal parameters, while modeling with two residual hexane molecules gave much more evenly distributed thermal parameters. Although these two molecules seemed to have a close van der Waals contact, it would not happen in reality, since these two residual molecules are in fact only one molecule which is disordered over two sets of positions. Except for those of the solvent molecules and part of the disordered amine ligand, hydrogen atoms were added with standard SHELXL idealizations. In the final refinement, bond length restraints were imposed on the disordered atoms. The structure was refined against F^2 by the SHELXL-93 program. The refinement converged to a final value of $R_1 = 0.1080$ and w$R_2 = 0.2460$ for observed unique reflections ($I \geq 2\sigma(I)$) and $R_1 = 0.1978$ and w$R_2 = 0.3064$ for all unique reflections including those with negative intensities. The weighted *R*-factors, wR_2, are based on F^2 and conventional *R*-factors, *R*, on *F*, with *F* set to zero for negative intensities. All reflections, including those with negative intensities, were included in the refinement and the $I \geq 2\sigma(I)$ criterion was used only for calculating R_1. The maximum and minimum residual electron densities on the final difference Fourier map were 0.481 and −0.360 e/Å^3, respectively. Final atomic coordinates are listed in Table S2′ (Supporting Information). The assignment of the correct enantiomorph was confirmed by the low value (0.04(4)) of the Flack absolute structure parameter[13] and the known chirality of the amine. The refinement of the enantiomorph in the space group $P6_2$ yielded a much higher Flack parameter, 0.48(5).

Results and Discussion

Synthetic Studies. The host molecule for the chiral amines used in this work was the metallochiroporphyrin CoCl(TMCP), **2**, prepared by oxidative insertion of $CoCl_2$ into the D_2-symmetric ($\alpha\beta\alpha\beta$) chiral ligand tetramethylchiroporphyrin in a mixture of chloroform−ethanol (4:1 v/v). The red/green diamagnetic complex **2** crystallized from dichloromethane−hexanes in 87% yield. The electronic absorption spectrum is typical of a five-coordinate Co(III) porphyrin in which all bands are bathochromically shifted, the α-band occurring at 612, the β-band at 570, and the Soret band at 449 nm. The ^{1}H NMR spectrum of **2** in CD_2Cl_2 is characteristic of a C_2-symmetric

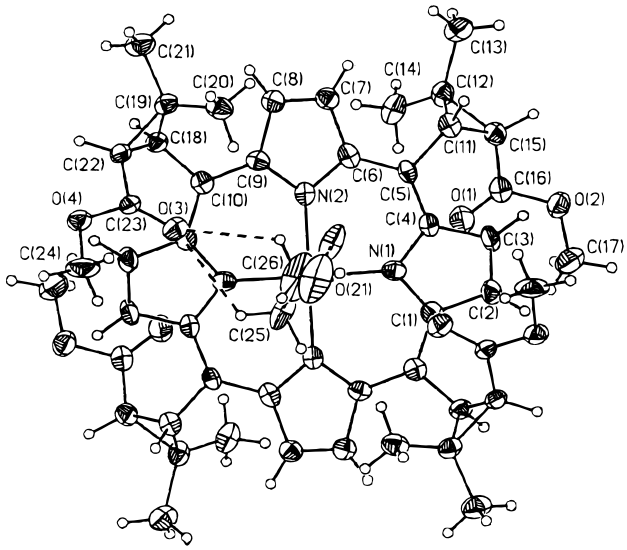

Figure 1. ORTEP diagram of [CoCl(OHCH$_2$CH$_3$)(TMCP)], view perpendicular to the porphyrin mean plane, showing the atom-labeling scheme. Thermal ellipsoids are drawn at the 30% probability level for the structure determined at 173 K.

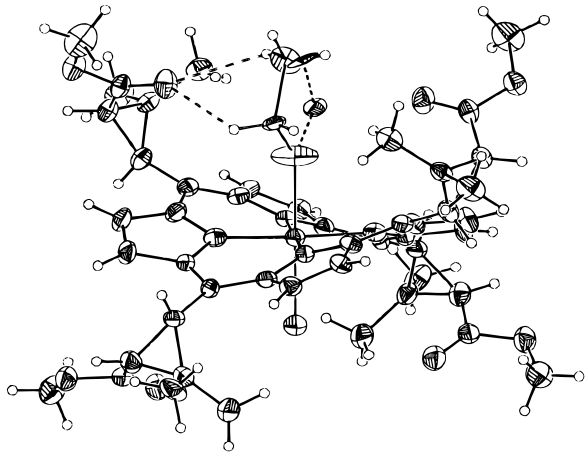

Figure 2. ORTEP diagram of [CoCl(OHCH$_2$CH$_3$)(TMCP)], side view showing the 2-fold disorder of the ethanol axial ligand and the two hydrogen bonds from the methylene and methyl groups to a carbonyl group for one of the two sites.

$\alpha\beta\alpha\beta$-metallochiroporphyrin, indicating that isomerization of the chiral ligand has not occurred during cobalt insertion. The presence of the axial chlorine atom renders the two faces of the porphyrin stereochemically inequivalent, resulting in two β-pyrrole multiplets at 9.34 and 9.22 ppm and two sets of distinct signals for the chiral *meso* substituents. Detailed spectral assignments are given in the Experimental Section.

X-ray Structures of [CoCl(OHCH$_2$CH$_3$)(TMCP)] and [Co(*(S)*-2-butylamine)$_2$(TMCP)][CoCl$_4$]$_{0.5}$. Figure 1 shows an ORTEP diagram of [CoCl(OHCH$_2$CH$_3$)(TMCP)] molecule viewed down the C_2 axis and the labeling scheme for the molecule. Figure 2 is a side view of the molecule, illustrating the six-coordinate cobalt atom at the center of the ruffled porphyrin and the disorder of the ethanol molecule. The bis adduct of [Co^{III}(TMCP)] with *(S)*-2-butylamine is illustrated in Figures 3 and 4. The two orientations of the disordered amine, found on the bottom face of Figure 3, are shown. The *(S)*-2-butylamine ligand on the top side is completely ordered. Figure 4 is a side view of the molecule showing the tetrachlorocobaltate anion and the water molecule. A complete complex consists of the six-coordinate species and half a $CoCl_4^{2-}$ counterion.

(12) Programs used in this study included: SHELXS-86 (Sheldrick, G. M. *Acta Crystallogr., Sect. A* **1990**, *46*, 467), SHELXL-93 (Sheldrick, G. M. *J. Appl. Crystallogr.*, in preparation), and local modifications of Johnson's ORTEP2. Scattering factors were taken from: *International Tables for Crystallography*; Wilson, A. J. C., Ed.; Kluwer Academic Publishers: Dordrecht, The Netherlands, 1992; Vol. C.

(13) Flack, H. D. *Acta Crystallogr., Sect. A* **1983**, *39*, 876.

Table 1. Crystallographic Data for [CoCl(OCH$_2$CH$_3$)(TMCP)] and [Co(*(S)*-2-butylamine)$_2$(TMCP)](CoCl$_4$)$_{0.5}$(H$_2$O)(C$_6$H$_{14}$)$_{0.5}$(CH$_2$Cl$_2$)$_{0.27}$

	[CoCl(OCH$_2$CH$_3$)(TMCP)]	[Co(*(S)*-2-butylamine)$_2$(TMCP)](CoCl$_4$)$_{0.5}$(H$_2$O)(C$_6$H$_{14}$)$_{0.5}$(CH$_2$Cl$_2$)$_{0.27}$
formula	$C_{50}H_{58}N_4O_9CoCl$	$C_{118.54}H_{167.09}Cl_{5.09}Co_3N_{12}O_{18}$
fw	953.38	2405.60
cryst system	tetragonal	hexagonal
a, Å	13.3540(2)	31.552(4)
b, Å	13.3540(2)	31.552(4)
c, Å	26.0422(2)	12.9241(13)
V, Å^3	4644.1(1)	11 143(2)
space group	$P4_32_12$	$P6_4$
Z	4	3
D_c, g/cm^3	1.362	1.075
radiation, Å	0.710 73	0.710 73
μ, cm^{-1}	4.88	4.78
temp, °C	−100(1)	−143(2)
R_1[a]	0.0604	0.1081
wR_2	0.1269	0.2464

[a] $R_1 = \sum||F_o| - |F_c||/\sum|F_o|$ and $wR_2 = \{\sum[w(F_o^2 - F_c^2)^2]/\sum[wF_o^4]\}^{1/2}$. The conventional *R*-factors R_1 are based on *F*, with *F* set to zero for negative F^2. The criterion of $F^2 < 2\sigma(F^2)$ was used only for calculating R_1. *R*-factors based on F^2(wR_2) are statistically about twice as large as those based on *F*, and *R*-factors based on all data will be even larger.

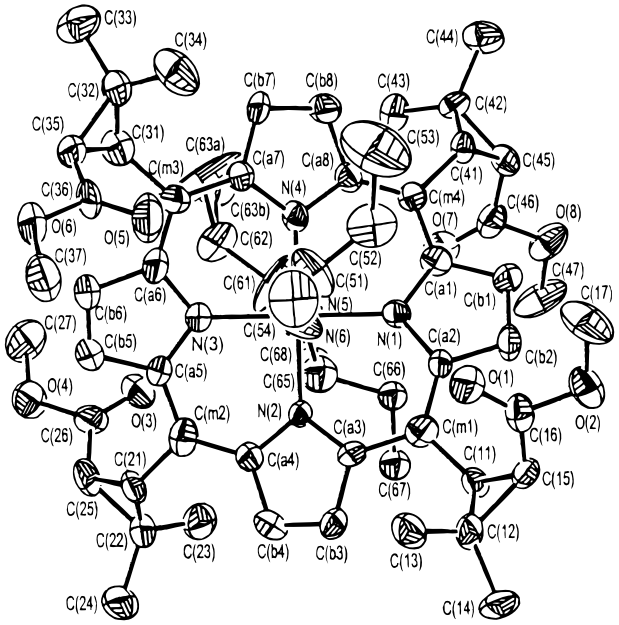

Figure 3. ORTEP diagram of [Co(*(S)*-2-butylamine)$_2$(TMCP)]-[CoCl$_4$]$_{0.5}$, view perpendicular to the porphyrin mean plane, showing the atom-labeling scheme. The two orientations of the disordered amine on the bottom face are shown. The *(S)*-2-butylamine ligand on the top side is completely ordered. Thermal ellipsoids are drawn at the 50% probability level for the structure determined at 130 K.

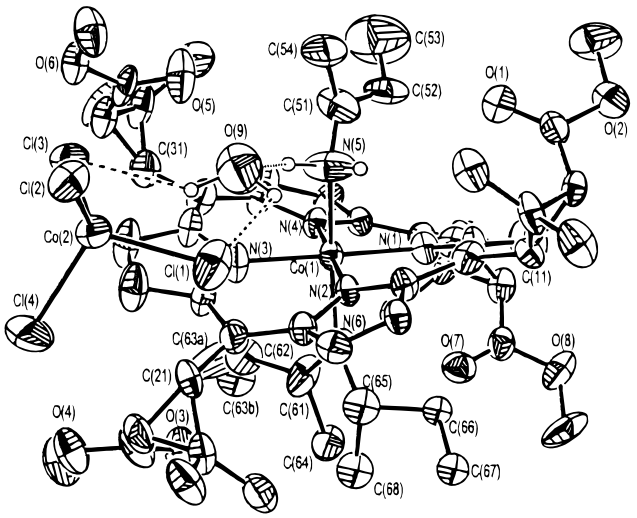

Figure 4. ORTEP diagram of [Co(*(S)*-2-butylamine)$_2$(TMCP)]-[CoCl$_4$]$_{0.5}$, side view showing the water molecule hydrogen-bonded to the amine group and to the tetrachlorocobaltate anion.

The latter presumably originates from adventitious $CoCl_2$ in the CoCl(TMCP) starting material. Tables 1 and 2 give the crystallographic details and a list of selected bond distances and angles, respectively, for both structures. Complete listings of bond distances and angles are included in the Supporting Information.

The porphyrin rings in derivatives **2** and **3** are both strongly ruffled in order to accommodate the alternating up, down *meso*-cyclopropyl substituents. The out-of-plane displacements from the 24-atom macrocyclic core for the two unique *meso* carbon atoms in **2** are 0.74 Å for C_5 and −0.74 Å for C_{10}, which are the largest yet found in a metallochiroporphyrin structure.[6,14] The displacements of the four *meso* groups in **3** are slightly smaller at −0.59, 0.61, −0.65, and 0.68 Å. The angle between adjacent pyrrole rings of porphyrin **2** is about 32°, while the average in **3** is 28°.

The methyl ester groups in **2** and **3** lie on the porphyrin ring with the carbonyl oxygen atoms nearly eclipsing the four α-pyrrole carbons. The carbonyl and one methyl of the *gem*-dimethyl group in two opposite cyclopropyl groups thus define a C_2-symmetric groove which accommodates an axial ligand on each face of the porphyrin.

The cobalt atom in **2** is slightly displaced from the porphyrin mean plane toward the chlorine atom (0.06 Å). The ethanol opposing the axial chloride ligand is held inside the porphyrin groove by a three-point interaction: a weak Co−O bond (2.048(8) Å) and two hydrogen bonds from the methylene and methyl group (C(25B)−H···O$_3$ 3.12(3) Å, *CH*$_2$; C(26A)−H···O$_3$ 3.07(3) Å, *CH*$_3$) to a carbonyl oxygen atom. The ethanol ligand is disordered with both the methylene and methyl groups equally distributed over the C_2-related sites. The coordinated oxygen atom is at 3.576 Å from O$_3$ and could be involved in a third, very weak hydrogen bond from the hydroxylic group, which presumably explains why this oxygen atom is not significantly displaced from the C_2 axis. In contrast, the X-ray structure of the isostructural ruthenium analog Ru(CO)(OCH$_2$CH$_3$)(TMCP) shows a slightly different conformation of the ethanol ligand,

(14) Mazzanti, M.; Marchon, J. C.; Wojaczynski, J.; Wolowiec, S.; Latos-Grazynski, L.; Shang, M.; Scheidt, W. R. *Inorg. Chem.*, submitted for publication.

Table 2. Selected Bond Distances (Å) and Angles (deg) for [CoCl($OHCH_2CH_3$)(TMCP)] and [Co(*(S)*-2-butylamine)$_2$(TMCP)]($CoCl_4$)$_{0.5}$(H_2O)(C_6H_{14})$_{0.5}$(CH_2Cl_2)$_{0.27}$

[CoCl($OHCH_2CH_3$)(TMCP)]		[Co(*(S)*-2-butylamine)$_2$(TMCP)]($CoCl_4$)$_{0.5}$(H_2O)(C_6H_{14})$_{0.5}$(CH_2Cl_2)$_{0.27}$	
		Lengths	
Co−Cl	2.211(3)	Co(1)−N(1)	1.937(9)
Co−N(1)	1.921(5)	Co(1)−N(2)	1.945(8)
Co−N(2)	1.928(5)	Co(1)−N(3)	1.950(9)
Co−O(21)	2.048(8)	Co(1)−N(4)	1.964(9)
		Co(1)−N(5)	1.985(10)
		Co(1)−N(6)	2.023(10)
C(25B)−H···O(3)	3.12(3)	N(5)−H···O(9)	3.09(9)
O(3)−H(25B)	2.61(5)	C(51)−H···O(5)	3.30(9)
C(26A)−H···O(3)	3.07(3)	C(54)−H···O(5)	3.27(9)
O(3)−H (26A)	2.52(6)	O(9)···Cl(1′)	3.19(9)
		O(9)···Cl(3)	3.35(9)
		Angles	
N(1)−Co−N(1)	176.5(3)	N(1)−Co(1)−N(2)	89.4(3)
N(1)−Co−N(2)	90.7(2)	N(1)−Co(1)−N(3)	179.9(7)
N(1)−Co−O(21)	88.2(2)	N(2)−Co(1)−N(3)	90.8(4)
N(1)−Co−Cl	91.8(2)	N(1)−Co(1)−N(4)	90.3(4)
N(2)−Co−N(2)	178.0(3)	N(2)−Co(1)−N(4)	179.1(3)
N(2)−Co−O(21)	89.0(2)	N(3)−Co(1)−N(4)	89.6(4)
N(1)−Co−Cl	91.0(2)	N(1)−Co(1)−N(5)	90.4(5)
O(21)−Co−Cl	180.0(2)	N(2)−Co(1)−N(5)	87.0(4)
		N(3)−Co(1)−N(5)	89.5(6)
C(25)−H−O(3)	117(1)	N(4)−Co(1)−N(5)	93.9(4)
C(26)−H−O(3)	120(1)	N(1)−Co(1)−N(6)	87.5(4)
		N(2)−Co(1)−N(6)	89.7(4)
		N(3)−Co(1)−N(6)	92.5(5)
		N(4)−Co(1)−N(6)	89.4(4)
		N(5)−Co(1)−N(6)	176.1(5)

in which the hydroxyl and methylene groups are disordered on two sites related by the 2-fold axis.[6]

The ordered amine in complex **3** is held within the porphyrin groove by a network of weak interactions to the carbonyl groups (C(51)−H···O(5) 3.30 Å; C(54)−H···O(5) 3.27 Å). It is also hydrogen bonded to a water molecule (N(5)−H···O(9) 3.09 Å); in turn, the latter is hydrogen bonded to the $CoCl_4^{2-}$ counterion (O(9)···Cl(1′) 3.19 Å; O(9)···Cl(3) 3.35 Å), as illustrated in Figure 4. The presence of the bulky tetrachlorocobaltate anion on that face of the porphyrin probably inhibits the disorder which is observed on the other face.

The average Co−N distance in derivative **2** is 1.925(5) Å, while that in **3** is 1.949(11) Å. Both of these averaged distances are shorter than any observed previously for cobalt(III) porphyrin derivatives[15] and consistent with the fact that these derivatives are somewhat more ruffled than the most ruffled cobalt(III) porphyrin previously characterized. Thus for [Co(NO_2)(3,5-lutidine)(TPP)],[16a] where the *meso* carbon atoms are displaced by an average of 0.60 Å, the averaged Co−N distance is 1.954(4) Å. Two slightly less ruffled derivatives, [CoCl(OH_2)-(TPP)][16b] and [Co(OH_2)$_2$(TPP)]$^+$,[16c] have Co−N distances of 1.955(2) and 1.964(4) Å, respectively. The axial Co−Cl bond distance of **2** is 2.211(3) Å, comparable to other six-coordinate Co−Cl distances.[16b,d] That the Co−Cl distance is shorter in five-coordinate [Co(TPP)(Cl)] (2.149(6) Å)[16e] is evidence of a real interaction to the *trans* ethanol (Co−O = 2.048(8) Å in **2**. The axial Co−N distances of 1.986(10) and 2.025(10) Å in **3** are within the range observed in other cobalt(III) derivatives.[17] The values of these and other axial Co−N distances appear to reflect the steric bulk of the specific axial nitrogen donor.

^{1}H NMR Studies in the Presence of Chiral Amines. The binding of racemic or optically pure chiral amines to **2** was initially monitored at room temperature by ^{1}H NMR in CD_2Cl_2. Titration with 2 equiv of the amines 2-butylamine (*(R)*, *(S)*, or *(R,S)*), 2-pentylamine (*(R,S)*), or 2-heptylamine (*(R,S)*) resulted in formation of the complex salt [Co(L)$_2$(TMCP)]Cl (L = *(R)*-, *(S)*-, or *(R,S)*-amine), where both axial coordination sites are occupied by amine ligands. When the ratio of the added base to metalloporphyrin was 1:1 or 0.5:1, the NMR spectrum presented a mixture of the unreacted material **2** and the bis-complex salt [Co(L)$_2$TMCP]Cl. This ratio remained unchanged throughout the observation at 25° for 48 h; formation of the mono-ligated species via equilibrium was not detected by ^{1}H NMR.

The formation of the amine salts is accompanied by a change in effective symmetry from C_2 in **2** to D_2 as seen by the NMR spectra. The NMR profile consists of a single set of resonances for the *meso* substituents and two singlets for the β-pyrrole protons. The high symmetry of this pattern implies a fast chemical exchange process on the NMR time scale between symmetry-related conformers of the coordinated amine, for example fast rotation around the Co−N bonds, resulting in three effective C_2 axes along the porphyrin normal and each N−N diagonal. Similar rotational mobility has been observed in other cobalt(III) porphyrin[7c] and iron(III) chiroporphyrin systems,[18]

(15) (a) Scheidt, W. R. *Acc. Chem. Res.* **1977**, *10*, 339. (b) Byrn, M. P.; Curtis, C. J.; Khan, S. I.; Sawin, P. A.; Tsurumi, R.; Strouse, C. E. *J. Am. Chem. Soc.* **1990**, *112*, 1865.

(16) (a) Kaduk, J. A.; Scheidt, W. R. *Inorg. Chem.* **1974**, *13*, 1875. (b) Iimura, Y.; Sakurai, T.; Yamamoto, K. *Bull. Chem. Soc. Jpn.* **1988**, *61*, 821. (c) Masuda, H.; Taga, T.; Osaki, K.; Sugimoto, H.; Mori, M. *Bull. Chem. Soc. Jpn.* **1982**, *55*, 4. (d) Sakurai, T.; Yamamoto, K.; Seino, N.; Katsuta, M. *Acta Crystallogr.* **1975**, *B31*, 2514. (e) Sakurai, T.; Yamamoto, K.; Naito, N.; Nakamoto, N. *Bull. Chem. Soc. Jpn.* **1976**, *49*, 3042. (f) Endregard, M.; Nicholson, D. G.; Abraham, R. J.; Marsden, I.; Beagley, B. *J. Chem. Soc., Faraday Trans.* **1994,** *90*, 2775.

(17) (a) Scheidt, W. R.; Cunningham, J. A.; Hoard, J. L. *J. Am. Chem. Soc.* **1973**, *95*, 8289. (b) Riche, C.; Chiaroni, A.; Gouedard, M.; Gaudemer, A. *J. Chem. Res. (S)* **1978**, 32.

(18) Wolowiec, S.; Latos-Grazynski, L.; Mazzanti, M.; Marchon, J. C. *Inorg. Chem.* **1997**, *36*, 5761.

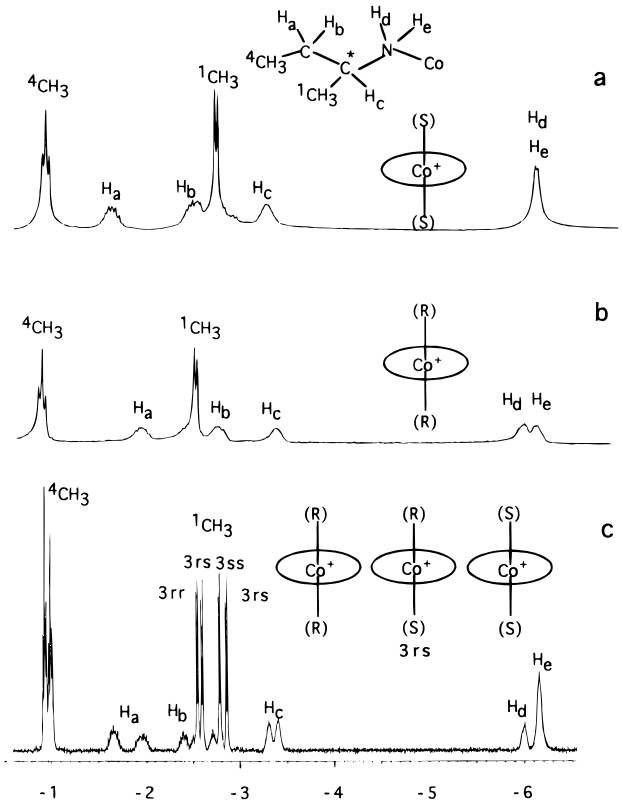

Figure 5. ^{1}H NMR spectra of the two 2-butylamine enantiomers coordinated to [Co^{III}(TMCP)] in CD_2Cl_2 at 25 °C: (a) *(S)*-2-butylamine at 200 MHz; (b) *(R)*-2-butylamine at 200 MHz; (c) *(R,S)*-2-butylamine at 400 MHz. The stereochemistry of the three cobalt(III) species and the proposed resonance attributions are indicated.

and it is reflected in the 2-fold disorder of one axial *(S)*-2-butylamine in the crystal structure of **3**.

Upon complex formation, the resonances of the amine protons are shifted upfield between 0 and −6.5 ppm, as a result of the strong shielding effect of the porphyrin moiety.[7] The shift is largest for those ligand protons nearest the macrocycle and whose location close to the porphyrin normal leads to an effective interaction with the ring current. The large dispersion of the upfield shifts (2−8 ppm) confirms that this ligand binds within the groove, and it indicates that exchange with free amine is slow on the NMR time scale at room temperature. The chiral nature of the host and slow-exchange kinetics result in a splitting of all diastereotopic protons. The observation of diastereotopic geminally coupled protons on C_β suggests the existence of noncovalent interactions between the chiral host and its guest, which freeze any rapid conformational equilibrium of the latter. The main interactions appear to be steric exclusion, which restricts the axial ligand to lie within the porphyrin groove along a *meso*−*meso* diagonal, and a network of weak N−H···O and C−H···O hydrogen bonds, as seen in the X-ray structure of **3** (*vide supra*). The combined effects of these interactions, and of the large porphyrin ring current, allow the ^{1}H NMR spectrum of the bound chiral amine ligand to be analyzed by first-order methods.

Figure 5a,b shows the distinct ^{1}H NMR profiles obtained at 200 MHz for the *(S)* and *(R)* enantiomers of 2-butylamine, respectively, bound to cobalt(III) as a bis(amine) complex salt. Notable spectral differences are observed, most prominently in the form of the signals observed for the diastereotopic protons of the NH_2 group. These appear as *two* broad, partially resolved singlets for the *(R)* enantiomer (−6.00, −6.14 ppm) and as *one* relatively narrow singlet for the *(S)* enantiomer (−6.13 ppm). Since the crystal structure of **3** shows that one of the two NH_2 protons is hydrogen-bonded to a water molecule, the observation of a single resonance for the *(S)* enantiomer complex in solution probably reflects fast exchange between the two chemically inequivalent NH_2 protons, or fast nitrogen inversion, on the NMR time scale. The spectra obtained with *(R,S)*-2-pentylamine and *(R,S)*-2-heptylamine showed a similar magnification of the chemical shift differences of the nonequivalent protons and gave characteristic spectroscopic patterns for the *NH* protons. The relatively narrow *NH* singlet seen in the NMR spectrum of the chiral amines of configuration *(S)* was in all cases located upfield from the two signals of the anisochronous protons of the NH_2 group of configuration *(R)*. Low-temperature NMR measurements on the *(S)*-2-butylamine complex did not resolve the relatively narrow singlet even at −80 °C, suggesting a low-energy barrier for the exchange process.

Figure 5a,b also presents the amine protons assignments as determined by DQF-COSY measurements. The two diastereotopic methylene protons H_a and H_b and the methine proton H_c located on the asymmetric carbon were unambiguously assigned; strong cross peak correlation was seen between the vicinal (*R*) protons H_a (−1.99) and H_c (−3.40) [H_a (−1.65) and H_c (−3.30); *(S)*] indicating their relative disposition along the propyl carbon chain. The strong H_a−H_c interaction was accompanied by very weak correlations between the (*R*) H_b (−2.8) and H_c (−3.4) [H_b (−2.5) and H_c (−3.3); *(S)*], confirming their conformation. Given the above spectroscopic profiles, the structural drawing on top of Figure 5 depicts the proposed proton assignments for the complex salts [Co(L)$_2$(TMCP)]Cl (**3rr**, L = *(R)*-2-butylamine; **3ss**, L = *(S)*-2-butylamine).

Replacing the *(S)* configuration with the *(R)* configuration—while maintaining the weak H_c···O═C interaction—interchanges the methyl group, $^1CH_3$, which is directed above the C_2 axis, with the ethyl group, $CH_aH_b{}^4CH_3$, which is directed over the porphyrin plane. This interconversion places the two substituents in very different magnetic environments, resulting in different shielding effects and different upfield shifts. This effect is readily seen by evaluating the complexation induced shift difference ($\Delta\delta$) defined as $\Delta\delta = \delta_s - \delta_r$. These values show that the largest chemical shift difference is for the protons H_a (0.34), H_b (0.24), and $^1CH_3$ (−0.24). For the resonance of H_c, the low value obtained for $\Delta\delta$ (0.11) can be explained by the solid-state structure of **3** (*vide supra*) which suggests the presence of a weak H_c···O═C hydrogen bonds to the carbonyl function in the porphyrin groove resulting in a relatively fixed position of the H_c proton in either the (*R*) or (*S*) enantiomeric form.

When 2 equiv of racemic *(R,S)*-2-butylamine was added to CoCl(TMCP), **2**, the ^{1}H NMR spectra showed a mixture of the three diastereomeric complexes [Co(LL′)(TMCP)]Cl (L = L′ = *(R)*-2-butylamine, **3rr**; L = L′ = *(S)*-2-butylamine, **3ss**; L = *(R)*-2-butylamine, L′ = *(S)*-2-butylamine, **3rs**). The abundance of **3rs** is twice that of either **3rr** or **3ss**, which are formed in approximately equal quantities.

Figure 5c presents an enlargement between 0 and −7 ppm of the 400 MHz ^{1}H NMR spectra for the upfield bound amine resonances of the racemic mixture. The resonances attributed to **3rr** and **3ss** can be readily identified; it appears that most of the resonances of the mixed complex **3rs** are superimposed with them. Thus, the signals of the (*R*) amine in **3rs** overlap with those of **3rr**, and the signals of the (*S*) amine in **3rs** overlap with those of **3ss**. The only resonances detectable for **3rs** are those attributed to the two independent methyl groups $^1CH_3$ located on the asymmetric carbon of the amine (*S*) and the amine

(*R*). These two methyl groups are equally coupled to H_c (J = 6 Hz) resulting in two sharp, well-resolved doublets at −2.59 and −2.87 ppm, *ca.* 0.06 ppm upfield of the equivalent methyl resonance associated with **3rr** and **3ss**. The detection of all four possible doublets in this region is undoubtedly due to the larger chemical shift difference and the small line width associated with the methyl $^1CH_3$ resonances ($\Delta\delta = -0.24$). Integration of the four observable methyl resonances gave **3rr**:**3ss**:**3rs** molar ratios of 1:1:2 for the three complexes. These ratios indicate that the three diastereoisomers are formed in statistical proportions, with no detectable influence of the chiral superstructures of metalloporphyrin **2** on the binding of the two enantiomers.

Axial Ligand Exchange Kinetics. This lack of enantioselection by cobalt(III) tetramethylchiroporphyrin is at first surprising, given the notable enantioselectivity (*ca.* 2:1) in favor the (*R*) enantiomer of (*R*,*S*)-2-octanol and (*R*,*S*)-2-butanol exhibited by the corresponding carbonylruthenium(II) complex, which is derived from the same chiroporphyrin.[6] Both metal complexes have the potential of discriminating axially bound enantiomers by three-point interaction on the basis of similar sets of noncovalent interactions; yet only the ruthenium complex exhibits enantioselective axial ligand binding. We suggest that the origin of this difference resides mainly in the kinetics of axial ligand dissociation from the two metal centers. In the ruthenium(II) chiroporphyrin complex, the strongly bound axial carbonyl labilizes the *trans* 2-octanol ligand, resulting in fast exchange on the NMR time scale at room temperature. Gradually lowering the temperature slows down ligand exchange and results in the appearance of distinct resonances for free and bound 2-octanol. At −70 °C the ^{1}H NMR spectrum reflects a thermodynamic equilibrium in which the two 2-octanol enantiomers exhibit distinct binding constants to the host, integrating the subtle influence of the chiral superstructures of the porphyrin. In marked contrast, amine binding to the cobalt(III) chiroporphyrin complex is essentially irreversible, and ligand dissociation is very slow on the NMR time scale at room temperature.[19] Thus, the ^{1}H NMR spectrum reflects the statistical binding of the two enantiomers on cobalt(III) on both faces of the chiroporphyrin, which does not integrate the influence of secondary interactions with the chiral superstructures, and kinetic control is observed (Figure 6).

We also note that the intramolecular hydrogen bonds to the amine ligand, which are seen in the crystal structure of **3**, probably also contribute to the slow axial ligand dissociation rate. Thus, it has been reported recently that in *Ascaris suum* oxyhemoglobin the bound dioxygen ligand is stabilized by hydrogen bonding from tyrosine residues.[20a] The same bonding pattern has been found in the oxygen-avid oxymyoglobin from

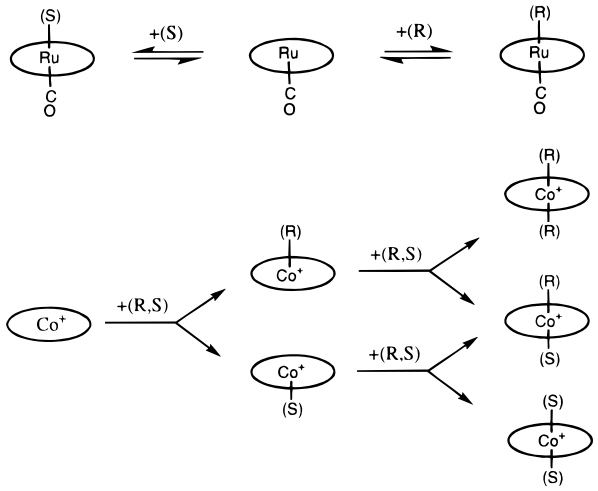

Figure 6. Schematic depiction of thermodynamic (top) versus kinetic (bottom) control of chiral ligand binding in metal complexes of tetramethylchiroporphyrin.

Paramphistomum epiclitum,[20b] and similar effects have been noted for the sulfide ligand in *Lucina pectinata* hemoglobin.[20c] In every case, this hydrogen-bonding stabilization is reflected in extremely slow dissociation rates of the axial ligand.

Potential Analytical and Enantioseparative Applications. Since kinetic control accurately reflects the concentrations of the free enantiomer ligands in solution, we believe that analytical applications, such as the determination of enantiomer composition, should be possible with this type of inert chiral Co(III) metallohost. The above results also show that the presence of transition metal centers in a chiral host brings an additional, powerful dimension to chiral recognition. Indeed, changing the metal center in a chiral host, such as tetramethylchiroporphyrin, offers the possibility to tune not only the binding constants of guests but also their exchange kinetics. Thus one can envision the possibility of using the same complexing chiral structure to design various useful reagents: chiral selectors with labile metal centers for enantioselection and separation[21] and nonselective chiral additives with inert metal centers for analysis.

Acknowledgment. J.-C.M. wishes to thank Professor James P. Collman for his generous hospitality at Stanford University, where this paper was written, and Professor Owen Curnow for an interesting discussion.

Supporting Information Available: A full ^{1}H NMR spectrum (10 to −7 ppm) of $[Co^{III}L_2(TMCP)]^+$ (L = *rac*-2-butylamine), Table S1, listing complete crystallographic details, Table S2, listing atomic coordinates and isotropic displacement parameters, Table S3, listing bond lengths and angles, Table S4, listing anisotropic displacement parameters for [CoCl(OHCH$_2$CH$_3$)(TMCP)], Table S1′, listing complete crystallographic details, Table S2′, listing atomic coordinates and thermal parameters, Table S3′, listing bond lengths, Table S4′, listing bond angles, Table S5′, listing anisotropic displacement parameters, and Table S6′, listing hydrogen coordinates and isotropic displacement parameters for [Co(*(S)*-NH$_2$CH(CH$_3$)CH$_2$CH$_3$)$_2$(TMCP)]-[CoCl$_4$]$_{0.5}$(H$_2$O)(C$_6$H$_{14}$)$_{0.5}$(CH$_2$Cl$_2$)$_{0.27}$ (29 pages). Ordering information is given on any current masthead page.

IC970995V

(19) That this system is not at equilibrium is also shown by the fact that no reaction is observed on addition of hydrochloric acid. Irreversible binding of (2-phenylethyl)amine and 3- and 4-aminoheptane to a d^6 chlororhodium(III) porphyrin has been also described. See: Aoyama, Y.; Yamagishi, A.; Asagawa, M.; Toi, H.; Ogoshi, H. *J. Am. Chem. Soc.* **1988**, *110*, 4076.

(20) (a) Huang, S.; Huang, J.; Kloek, A. P.; Goldberg, D. E.; Friedman, J. M. *J. Biol. Chem.* **1996**, *271*, 958. (b) Zhang, W.; Ka, R.; Haque, M.; Siddiqi, A. H.; Vinogradov, S. N.; Moens, L.; LaMar, G. N. *J. Biol. Chem.* **1997**, *272*, 3000. (c) Rizzi, M.; Wittenberg, J. B.; Coda, A.; Ascensi, P.; Bolognesi, M. *J. Mol. Biol.* **1996**, *258*, 1.

(21) See for example: Allen, P. R.; Reek, J. N. H.; Try, A. C.; Crossley, M. J. *Tetrahedron Asymmetry* **1997**, *8*, 1161.